

## EMI Testing Using Metallic Enclosure – A Case Study

*R. Seetharaman, R. Vandana, K. Venkata Srinath, and S. Babu*

Department of Electronics and Communication Engineering,  
College of Engineering, Guindy,  
Anna University, Chennai-600025, India

Copyright © 2016 ISSR Journals. This is an open access article distributed under the **Creative Commons Attribution License**, which permits unrestricted use, distribution, and reproduction in any medium, provided the original work is properly cited.

**ABSTRACT:** A test setup has been devised here to quantify EMI. The frequency range of operation is proposed in GHz range. Measurement of internal fields via antennas is taken as a parameter for characterising interaction between digital components. For low frequencies MoM and FEM solvers is apt for simulation purposes. For high frequencies statistical approach has been chosen. Using these techniques real components are being reproduced as simplistic geometric models. This setup can be further extended to real time PC casing.

**KEYWORDS:** Electromagnetic compatibility (EMC), electromagnetic measurements, enclosures.

### 1 INTRODUCTION

Byzantine digital systems resorting to high frequency ranges makes EMI a prevalent aspect of concern. Predicting EMI at these frequencies is unfeasible. Especially for shielding enclosures with, intricate EM fields and dampened resonances this is an issue. As electronic equipments are becoming much more smaller, quantifying EMI and ascertaining its sources has a high end priority at design and testing

Typifying metallic cavities using numerical modelling is a tedious task. Large number of unknowns and computation times makes it quite inappropriate for proficient modelling. Analytical methods such as closed form EMI estimate [1],[2] have been developed. All these methods pertain to simple rectangular cavities and aperture composition. Physically small electrically large enclosures modelling involving reverberation chambers [3],[5] are popular approaches used these days. S parameter determination by frequency stirring [6],[8] and averaging the power level inside the enclosure makes shielding effectiveness problem undemanding. A prologue of the test setup is illustrated here.

A block level implementation is exemplified in fig 1. A metallic enclosure mounted by 12 short monopole antennas is used. Affixing SMA connectors at the exteriors of antennas facilitate them to act as probes. The interaction between antennas and metallic cavity is assessed using a 12-port vector network analyser [9],[10].

Fast and efficient MoM (Method of Moments) [11] approach is typically preferred here as it is both applicable low as well as high frequencies in statistical investigations. Whole PC casing volume is considered for test setup allowing study of coupling between internal components. The paper has been devised into 4 sections. Initially preface to setup is given. Effect of antenna factor, arrangement for analytical and numerical validity of test setup followed by modelling of internal components in PC casing is illustrated.

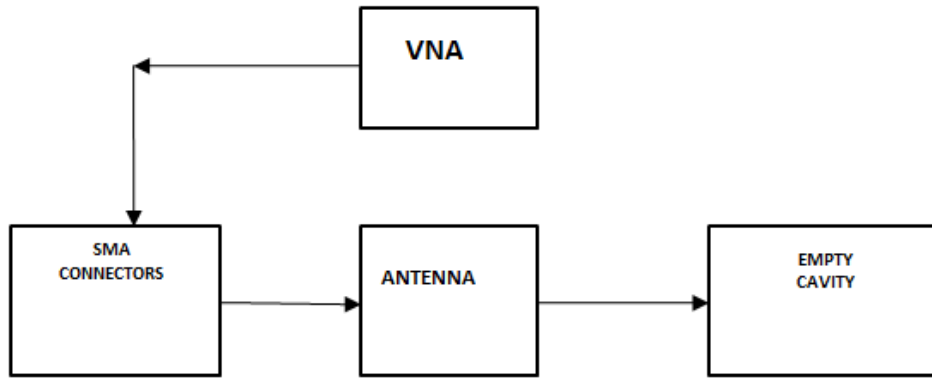


**Fig.1 Block diagram of experimental setup. Components include 12 port VNA, SMA connectors antenna and empty cavity. SMA connectors and antenna find input feed part.**

## 2 TEST SETUP

First of all, an aluminium cavity with dimension similar to PC casing should be constructed with specific thickness. The front plate of cavity has to be made exchangeable to analyse different situations in PC casing such as apertures, cables and allows to place components inside which can be tightened with help of screws to casing. Inset shielding gasket can be used between plate and casing for EM energy leakage prevention.

Radiation sources such as extra cables can disturb cavity setup. So, SMA connectors protruded inside are used as antennas wherein this specific length can be determined. The dielectric coating of SMA connectors be removed to form monopole antennas where length= $l_a$ . These are used as electric field probes to measure internal fields which are connected to 12 port network analyser.

The probes will be considered as ports and connected to VNA. The coupling between antennas allows characterizing internal components interaction. Ports are not placed at bottom because this space is allocated for placing components inside cavity. Probe orientations need to be convenient such that at every point inside cavity electric field can be measured.

With the help of this setup, we need to prove the internal fields due to antennas inside cavity can be well correlated with the interaction of digital components inside. The interaction of antennas is measured by an impedance matrix or Z parameters by MoM solver [12]. Here we can construct a plot for impedance of any two ports vs. frequency in GHz.

For validation of setup measurements can be repeated for dipoles of length  $l_d=2l_a$  located at the same antenna ports cavity in x, y and z direction. As considered for antenna impedance parameters, voltage at input ( $V_p$ ) of dipole and current  $I_p$  need to be calculated. This obtained “*impedance*” can henceforth be compared with the antenna parameters obtained. To obtain a graphical conclusion port excitations and dipole validation is to be compared for maximum interaction vs. frequency with the help of MoM simulations. Thus obtained results will only allow us to conclude for using antenna parameters as performance factor for EMI inside cavity.

## 3 ANTENNA IMPACT

Obtaining a correlation between internal electric fields and antenna parameters entails a figure of merit. This parameter defined as antenna factor (k) obtained from Z-parameter configuration is characterized by [13]:

$$k = \frac{|E_p|}{V_p} = \frac{1}{l_{eff}} \quad (2)$$

First resonant frequency of these monopole antennas ascertains maximum permissible operational frequency range. The finite ground plane assumption for monopole antennas contradicts linear current distribution over its entire length. To substantiate this fact, a source (dipole) is placed interior to the cavity. Dipoles can be oriented in any arbitrary direction. The subsequent voltage  $V_p$  at ports should be observed. Without monopoles fields are to be evaluated at antenna feed points. Electric field intensity  $E_p$  at first port should be compared with analogous port voltage. The outcomes should be consistent. Amplitudes at resonant frequencies may differ due to antenna mismatch. Dipoles can be oriented in any arbitrary direction.

3.1 IMPEDANCE COUPLING FOR ANTENNAS

Validation of the test setup necessitates analytical approach. Presuming dipoles to be oriented in z direction, where  $l_1$  and  $l_2$  are lengths of antenna  $l_x$ ,  $l_y$  and  $l_z$  dimensions in x y and z direction notably located at positions  $r_a$  and  $r_b$  the coupling impedance denote as  $Z_{12}$  [14] can be written as:

$$Z_{12} = \frac{j\omega\mu}{2k\sin(kl_2/2)} [G_{ZZ}^A(r_a, r_b + l_1/2e_z) - G_{ZZ}^A(r_a, r_b - l_1/2e_z)] 2\cos(kl_1/2)(r_a, r_b) \int_{antenna2} S_1(r^{(2)}) (dr^{(2)}) \tag{3}$$

$$G_{ZZ}^A(r, r') = \sum_{m=1}^{\infty} \sum_{n=1}^{\infty} \sum_{p=0}^{\infty} \left[ \frac{\epsilon_0 p}{l_x l_y l_z} \cdot \sin\left(\frac{m\pi x}{l_x}\right) \sin\left(\frac{m\pi x'}{l_x}\right) \sin\left(\frac{n\pi y}{l_y}\right) \sin\left(\frac{n\pi y'}{l_y}\right) \cos\left(\frac{p\pi z}{l_z}\right) \cos\left(\frac{p\pi z'}{l_z}\right) \right]$$

$$\left(\frac{m\pi}{l_x}\right)^2 + \left(\frac{n\pi}{l_y}\right)^2 + \left(\frac{p\pi}{l_z}\right)^2 - k^2 \tag{4}$$

Where  $\left(\frac{m\pi}{l_x}\right) = k_x$ ,  $\left(\frac{n\pi}{l_y}\right) = k_y$ ,  $\left(\frac{p\pi}{l_z}\right) = k_z$   $\epsilon_0 p = 1$  for  $p=0$  or is 2

$G_{ZZ}^A$  is Green's function for a cavity [15], [16], k is wave number of material with permeability  $\mu$

Mathematical nature of Green's function makes the rate of convergence slow. Accelerating the rate of Green's function is a prerequisite here.

Antenna input impedance can be expressed as:

$$Z_{ip} \approx R_{rad} + \frac{1}{j\omega C} \tag{5}$$

Capacitance C part of imaginary part of the input impedance is static capacitance facing wall.

Where  $R_{rad} = 0$  considering cavity as lossless. Complete impedance matrix of two antennas is calculated. Any arbitrary antenna configuration can be derived here [16]. Considering infinite ground resonance effects can be neglected.

4 MODELLING TRANSITION FROM CABLE TO ANTENNA FEED

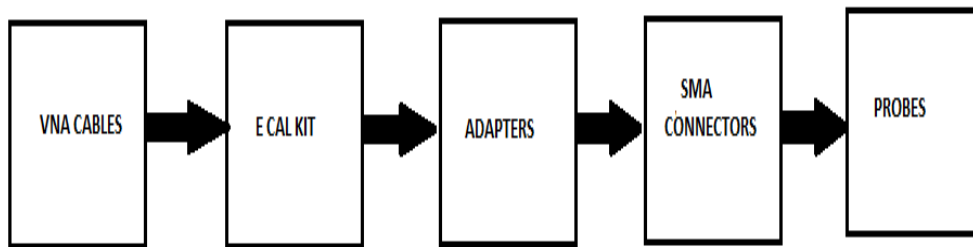


Fig.2. Block diagram from VNA cables to probe transition.

The block diagram in Fig.2 shows VNA cable connections to antenna input. VNA is connected to test setup through VNA cables. SMA connectors are connected to field probes so adapter is apt. An ECal [17] mechanical standard kit is available which can be attuned to the end of adapters. SMA connectors and cable extension inside chassis wall has not been taken into consideration till now. These represent added radiation issues and proper lengths need to be calculated for shifting the reference plane (inner side of front plate) accordingly. So, a complete adjustment of kit to reference plane cannot be done here.

All the twelve ports need to be connected to this reference plane using the kit so reference plane has to be changed accordingly to negate such issues. This complete changeover from cable to antenna feed is to be modelled in terms of error network E [18]. Complete analysis includes first conversion of Z-parameters to S-parameters. Error coefficients are obtained from above mentioned error network.

A plot should be constructed corresponding to phase of any one port against simulated setup vs. frequency in GHz range. The phase shift mainly occurs due to adapter and connectors. Determining parameters from slope of above graph provides us with the necessary length needed.

The electric length from cable to inner side can be obtained and shifted appropriately using error network. The length for all other ports should also be same. After shifting the reference plane, S-parameters can be converted to Z-parameters for better comparisons [19]

## 5 DISCUSSION RESULTS

Full wave solvers will not be advantageous here for simulations due to high inefficiency. Finite Integration Method [20] is also not suitable as convergence issues are involved. FEM (Finite Element Method) [21] and H- matrix MoM (Method of Moments) can be effective in these cases as computational efficiency is high. Both can yield comparable results. FEM solver method requires 'air-box' if apertures are present. But H-MOM [12], [22] solver does not involve such limitations and can be used throughout this setup as an excellent solver.

## 6 HIGH FREQUENCY RANGE APPROACH

Inverse cubic relationship of mode density vs. frequency makes numerical modelling inappropriate. Furthermore, finer sampling would be needed which validates the necessity of statistical analysis. Wavelength dimensions become comparatively smaller with increasing frequencies affecting electrical characteristics of shielding enclosures. Therefore, interpretation of multimode cavity in terms of statistical approach is desired. Orientation of electric field is measured by locating probes in x, y and z direction removing port dependence. Dominant mode inside cavity determines coupling at particular frequencies.

High Q factor cavities tend to be more prone to resonant frequency deviations. So, sampling effect is predominant in determining mutual interactions between chassis components.

The p-quantile of CDF (Cumulative Distribution Function  $F_X$  of variable X is [23] :

$$Q_X(p) = \inf \{x \in \mathbb{R} \mid F_X(x) \geq p\}, \text{ with } p \in (0, 1) \quad (6)$$

The percentiles are interrelated to quantiles by  $P_X(p) = Q_X(p/100)$ . The CDF of the function requires elements from S-matrix is to be taken. Here we can assume 90% confidence interval of S parameter percentile for graphical observations.

The behaviour of cavity can be illustrated graphically for different frequency regions where a comparison of 90% confidence intervals of S-parameters vs. frequency should be plotted. Here we will divide graph into three regions 1) low frequency region till 2.5 GHz 2) Intermediate region 3) High frequency region. Low frequency and intermediate regions can be analysed by H-MoM method. As stated earlier large number of resonances occurs in high frequency region so noise can readily occur. Any deviations accompanied here can be accounted in equivalent Q factor ( $Q_{eff}$ ) as background losses [19].

$$\tan \delta_e = \frac{1}{Q_{eff}} \quad (7)$$

For measuring  $Q_{eff}$  again graphical illustration for 90% confidence intervals vs. frequency (GHz) for cavity measurement should be done with finer frequency sampling of suppose 1kHz in high frequency range from where Q factor for closed cavity can be determined.

## 7 REPLACEMENT OF INTERNAL COMPONENTS

Factual pc's enclosures are usually multifaceted wherein entities such as circuit power supply cables increase EM field complexity. Therefore, precise modelling of PC geometry is unrealistic. This section provides an insight into a rough modelling of internal components inside PCS. Simple layouts have been used to these modelling. These models are particularly used for assessing the effect on field distribution of a cavity. A motherboard usually has been used with cards/metal plates and heatsinks placed above it.

### 7.1 PCB's

Thin sheet approximation of a PCB due to surface current phenomenon allows modelling of PCB as thin metallic plates [24], [25]. The replica PCB setup considered consists of cards placed perpendicular to motherboard. Two varieties of cards are used here. The first is made of copper stratum on lossy conductive Milliken substrate .The second one used here is aluminium. For convenience thickness is assumed to be same 2mm. Cards are separated by EPS (Expanded polystyrene) which resemble properties of vacuum as shown in Fig.3

Initially as reference real PCB impact on closed cavity can be taken using MoM simulation where coupling impedance of antenna vs. frequency comparison can be emulated graphically. Subsequently motherboard/card configuration setup can be placed inside cavity. Both arrangements Millikan and aluminium can be examined. Mutually low and high frequency measurements should be carried out.

For high frequencies statistical approach needs to be performed. Here also graphical approach is done by placing dummy PCB setup inside enclosed cavity and comparing S-parameters vs. frequency using simulations. Dielectric losses are encountered in PCB's which may lead to high frequency deviations. The result obtained authenticates whether this dummy PCB setup as thin metal plates is valid replacement for real PCB's.

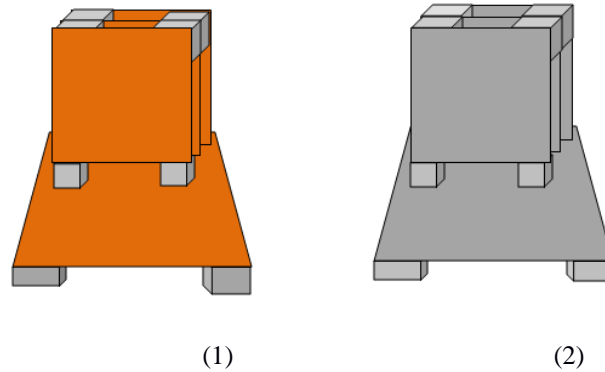


**Fig.3. Setup of cards on motherboard**

(1) replication of original model consisting copper cards on Millikan substrate.

(2) Aluminium cards on Millikan substrate. Both are of equal thickness.

## 7.2 HEATSINKS

An accurate outline of heatsink is too complicated. These are used for dissipation of heat in PCs. Their Structure is composed of heat spreaders and cooling fins. Usually these are replicated as PEC (perfect electrically conducting blocks)[ 26]- [ 28].To model as PEC case, Heat sink is enclosed with aluminium foil and fastened with tape with fan removed.(Fig 4)

Results from graphical setup will convey low and high frequency characteristics. Firstly, coupling impedance for antenna in presence of heatsink for closed cavity is carried out. The frequency influence can be studied in this way. Secondly, S-parameters are compared vs. frequency for heatsink model placed on motherboard both cases MoM simulation method is performed. This will corroborate whether PEC modelling of heatsink is apposite or not.

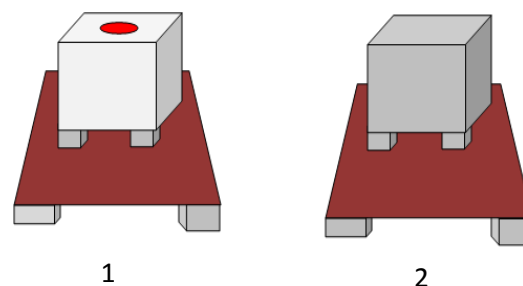


**Fig.4. Heatsink impact: (1) Without fan placed on motherboard. (2)Aluminium foil wrapped setup**

## 7.3 APERTURES

Various types of aperture compositions are used in PC casings. Penetration of external components, power cables, ventilation grids all are through apertures. Electrically small apertures (comparable wavelength dimensions) increase shielding effect. Practically the energy penetration is through apertures. Depending on the area and aperture number impact can be analysed. Front plate of chassis is interchanged by different plates having diverse constitution of apertures. First is

blind plate. Second one contains an array of circular approx 150 apertures illustrated in Fig 5. The third consists of long slots in vertical and horizontal direction. The aperture can be extended to one face of cavity which is the worst case of shielding estimate.

Here also graphical approach is done by comparing 90% confidence of S-parameters with frequency in GHz. All the three plates are examined for this frequency range.

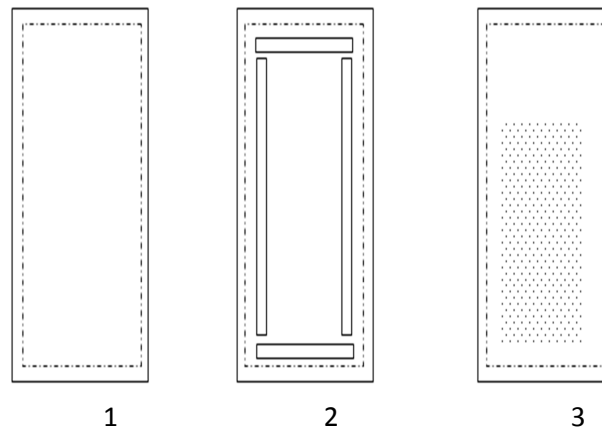


**Fig.5. Aperture configurations: (1) blind plate (2) with long thin slots (3) array of circular apertures containing approx 150 holes.**

#### 7.4 CABLES AND STRUCTURAL COMPONENTS

Here also these components are modelled as PEC surfaces. Structural components include disk drives etc. Here also Q factor pertaining relations are to be obtained. Additional components like cables connectors introduce losses which are embraced in background losses.

The results and prediction of the test setup can be acquired by following above mentioned standard procedures. Taking into guaranteed, the MoM solver provides best accurate solution simulations are performed. Impact of losses in chassis can also be inferred graphically at low and high frequency ranges.

#### 7.5 REALISTIC PC CHASSIS SETUP

The considered layout could be further extended to pragmatic PC setup with internal components. Here also SMA probes need to be connected. Simulations are carried out to measure Q factor for real PC setup and with internal components inside. We need to prove here whether real PC setup also gives the same simulation results in comparison to empty cavity.

90% confidence interval for empty cavity should be compared with empty cavity and one with internal components. If the PC chassis is smaller than setup, a shift to high frequencies may occur.

### 8 CONCLUSION

The proposed setup here is to measure EMI in metallic cavity. A metallic cavity similar to dimensions of PC casing has to be developed wherein the interaction of internal components are being characterized by the monopole antennas present on the cavity walls. For low frequency ranges MoM (Method of Moments) simulation method would be suitable for the setup. However, for high frequency measurements statistical approach has been used.

Simplified geometric replicated models for internal digital components can be constructed and validated .Q factor for empty cavity and containing components within it can be measured. High frequency ranges typically tend to lowering of q factor which can be included in background losses of the material. This setup can also be validated and extended to a real time office workstation. Thus coupling between antennas can be used as a performance factor to measure EMI inside cavity. This method thus proposed may be extended to any random configuration.

## REFERENCES

- [1] M. Robinson, T. Benson, C. Christopoulos, J. Dawson, M. Ganley, A. Marvin, S. Porter, and D. Thomas, "Analytical formulation for the shielding effectiveness of enclosures with apertures," *IEEE Trans. Electromagn. Compat.*, vol. 40, no. 3, pp. 240–248, Aug. 1998.
- [2] M. Li, J. L. Drewniak, S. Radu, J. Nuebel, T. H. Hubing, R. E. DuBroff, and T. P. Van Doren, "An EMI estimate for shielding-enclosure evaluation," *IEEE Trans. Electromagn. Compat.*, vol. 43, no. 3, pp. 295–304, Aug. 2001.
- [3] C. Holloway, D. Hill, M. Sandroni, J. Ladbury, J. Coder, G. Koepke, A. Marvin, and Y. He, "Use of reverberation chambers to determine the shielding effectiveness of physically small, electrically large enclosures and cavities," *IEEE Trans. Electromagn. Compat.*, vol. 50, no. 4, pp. 770–782, Nov. 2008.
- [4] R. Armstrong, A. Marvin, and J. Dawson, "Shielding effectiveness estimation of physically small electrically large enclosures through dimensional scaling," in *Proc. IEEE Int. Symp. Electromagn. Compat.* Aug. 2012, pp. 652–656.
- [5] L. Kovalevsky, R. Langley, and A. Barbarulo, "Method for determining statistical mean and variance of electromagnetic energy transmission between coupled cavities," in *Proc. IEEE Int. Symp. Electromagn. Compat.* Sep. 2014, pp. 1007–1011.
- [6] S. Hemmady, T. M. Antonsen, E. Ott, and S. M. Anlage, "Statistical prediction and measurement of induced voltages on components within complicated enclosures: A wave-chaotic approach," *IEEE Trans. Electromagn. Compat.*, vol. 54, no. 4, pp. 758–771, Aug. 2012.
- [7] G. Gradoni, V. Primiani, and F. Moglie, "Dependence of reverberation Chamber performance on distributed losses: A numerical study," in *Proc. IEEE Int. Symp. Electromagn. Compat.* Aug. 2014, pp. 775–780.
- [8] Z. Drikas, J. Gil Gil, S. Hong, T. Andreadis, J. Yeh, B. Taddese, and S. Anlage, "Application of the random coupling model to electromagnetic statistics in complex enclosures," *IEEE Trans. Electromagn. Compat.* vol. 56, no. 6, pp. 1480–1487, Dec. 2014.
- [9] Keysight Technologies, "N5225A PNA microwave network analyzer," Technical Specifications".
- [10] Agilent Technologies, Inc., "U3025AE10 50 GHz, 10-port mechanical test set," User's Guide, Mar. 2009.
- [11] V. Rajamani, C. Bunting, M. D. Deshpande, and Z. Khan, "Validation of modal/MoM in shielding effectiveness studies of rectangular enclosures with apertures," *IEEE Trans. Electromagn. Compat.* vol. 48, no. 2, pp. 348–353, May 2006.
- [12] Technische Universität Hamburg-Harburg. The CONCEPT-II website. (2015). [Online]. Available: <http://www.tet.tuhh.de/concept>
- [13] W. L. Stutzman and G. A. Thiele, *Antenna Theory and Design*. Hoboken, NJ, USA: Wiley, 2013.
- [14] F. Gronwald, "Antenna theory in resonating systems derived from fundamental electromagnetism," Germany, 2006.
- [15] J. West, V. Rajamani, and C. Bunting, "Practical considerations for the evaluation of the 3-D Green's function in a rectangular cavity moment method at high frequency," in *Proc. IEEE Int. Symp. Electromagn. Compat.* Aug. 2013, pp. 813–818.
- [16] M. E. Gruber, C. Koenen, and T. F. Eibert, "A fast Fourier transform accelerated Ewald summation technique for the vector electromagnetic rectangular cavity Green's function," *J. Comput. Phys.*, vol. 280, pp. 570–578, Jan. 2015.
- [17] Keysight Technologies, "N4693-60003 electronic calibration (ECal) modules," Reference Guide, Aug. 2014.
- [18] V. Teppati, A. Ferrero, and M. Sayed, *Modern RF and Microwave Measurement Techniques*. New York, NY, USA: Cambridge Univ. Press, Jul. 2013.
- [19] D. M. Pozar, *Microwave Engineering*. Hoboken, NJ, USA: Wiley, 2012.
- [20] CST Corporation. (2011). CST Microwave Studio (MWS) [Online]. Available: <http://www.cst.com>
- [21] ANSYS, Inc. (2014). HFSS [Online]. Available: <http://www.ansys.com>
- [22] A. Vogt, T. Reuschel, H.-D. Bruns, S. Le Borne, and C. Schuster, "On the treatment of arbitrary boundary conditions for a fast direct H-matrix solver in MoM," *IEEE Trans. Antennas Propag.*, submitted, Jan. 2015.
- [23] A. Vogt, H.-D. Bruns, Qi Wu, F. Gronwald and C. Schuster, "A measurement setup for quantification of electromagnetic interference in metallic casings" *IEEE Trans. Electromagn. Compat.*, Accepted Jun 2015.
- [24] X. Duan, A. Vogt, H.-D. Bruns, and C. Schuster, "Progress towards a combined CIM/MoM approach for EMI analysis of electronic systems," in *Proc. IEEE Int. Symp. Electromagn. Compat.* Sep. 2012, pp. 1–6.
- [25] M. Sorensen, I. Bonev, O. Franek, G. Petersen, and H. Ebert, "How to handle a Huygens' box inside an enclosure," in *Proc. IEEE Int. Symp. Electromagn. Compat.*, Aug. 2013, pp. 802–807.
- [26] J. Dawson, A. Marvin, S. Porter, A. Nothofer, J. Will, and S. Hopkins, "The effect of grounding on radiated emissions from heatsinks," in *Proc. IEEE Int. Symp. Electromagn. Compat.*, Aug. 2001, pp. 1248–1252.
- [27] D. Hockanson and R. Slone, "Investigation of EMI coupling at CPU interconnect," in *Proc. IEEE Int. Symp. Electromagn. Compat.*, Aug. 2004, pp. 424–429.
- [28] Z. Yu, J. Mix, S. Sajuyigbe, K. Slattery, D. Pommerenke, and J. Fan, "Heat-sink modeling and design with dipole moments representing IC excitation," *IEEE Trans. Electromagn. Compat.*, vol. 55, no. 1, pp. 168–174, Feb. 2013.